

Origin of low-friction behavior in graphite investigated by surface x-ray diffraction

Bing K. Yen^{ab} and Birgit E. Schwickert

IBM Almaden Research Center, 650 Harry Road, San Jose, CA 95120

Michael F. Toney

Stanford Synchrotron Radiation Laboratory, Stanford Linear Accelerator Center, 2575

Sand Hill Road, M/S 69, Menlo Park, CA 94025

Contrary to popular belief, the slipperiness of graphite is not an intrinsic property. The presence of vapors, such as water, is required for graphite to lubricate; in vacuum or dry environments, the friction and wear rate of graphite are high. A widely accepted explanation involves weakening of the binding force between basal planes near the surface, thereby allowing these planes to shear easily. This weakening results from proposed chemisorption or intercalation of vapor molecules near the surface, leading to an increase in the interlayer spacing between near-surface basal planes. Here we use X-ray diffraction from a synchrotron source to show that the basal plane spacing at the surface is the same in vacuum, ambient air, or water vapor saturated air. These results refute this long-held view that the low friction behavior of graphite is due to shearing of weakened basal planes.

Work supported in part by the Department of Energy Contract DE-AC03-76SF00515

^a Electronic mail: bing.yen@hgst.com

^b Present address: Hitachi GST San Jose Research Center, 650 Harry Road, San Jose, CA 95120

Graphite has long been recognized to be an effective dry lubricant, but its low-friction behavior was not well understood until W. Bragg first discovered its lamellar structure by x-ray diffraction in 1928,¹ whence began the long debate on this subject.²⁻¹² Figure 1 shows the highly anisotropic, layered crystalline structure of graphite, which has strong bonding within the basal planes but weak bonding between these planes as evidenced by the large spacing between them. Bragg attributed the slipperiness of graphite to the shearing of these weakly bonded basal planes.¹ This lattice-shear theory was generally accepted until graphite commutator brushes on high-flying aircraft in the late 1930s experienced abnormally high wear rates (10^3 - 10^4 times normal) owing to the low humidity at high altitude.² It was subsequently shown that in the absence of certain gases and vapors in the environment, such as water, O₂ and CO₂, graphite would exhibit this high friction and wear behavior,³ also known as “dusting.” Hence, the lubricity of graphite is not an intrinsic property, as implied by Bragg’s shear theory. Later Rowe attempted to reconcile the lattice-shear theory and the observed vapor dependency by proposing that vapors could enter into the graphite lattice and reduce the binding strength between basal planes.⁴ Such an intercalation reaction would result in the expansion of the lattice, but Arnell and Teer found no change in the interlayer spacing between graphite basal planes in *bulk* graphite samples, as measured by x-ray diffraction, when outgassed graphite was exposed to ambient atmosphere.⁵ Because of the limitation of their bulk diffraction technique, however, Arnell and Teer specifically pointed out that their experiments could not preclude the possibility that the interlayer bonding of the basal planes is weakened *only* near the graphite surface,⁵ which is the region of interest in the context of friction and wear. This surface effect could be due to intercalation of

vapor between the topmost layers⁴ (see Fig. 1d) or to chemisorption of vapor molecules onto the basal plane, which would weaken the top-layer bonding (π -electron bond etching,⁶ see Fig. 1c).

In contrast to Bragg's lattice-shear model, Deacon and Goodman attributed the slipperiness of graphite to its low surface adhesion forces when dangling bonds at the edge planes are saturated by chemisorbed vapor molecules.⁷ Consistent with this alternate adhesion model, researchers have found the friction at the edge planes, which are covered with dangling bonds, is high in vacuum.⁸ While recent experiments on the effect of various gases and vapors on the friction of graphite lend some collateral support to the adhesion theory,^{9,10} there is no direct evidence hitherto that could confirm or refute the validity of either theory. Hence, the lattice-shear theory and its modifications are still widely accepted.^{13,14}

The weakening of the interlayer bonding by vapor molecules, as proposed in the lattice-shear model, would lead to an increase in the basal-plane spacing at or near the graphite surface. To test this possibility, we have conducted surface X-ray diffraction measurements on c-axis (basal plane) oriented single crystal graphite in high vacuum ($<1 \times 10^{-3}$ Torr), in laboratory air (ca 50% humidity), and in water saturated air (nearly 100% humidity). The termination of a crystal at a surface produces X-ray scattering that is additional to the Bragg peaks of the crystal.¹⁵ These truncation rods are ridges of scattering that connect Bragg points and are sensitive to the topmost layers of the crystal, including adsorbed layers and intercalated layers. We have specifically measured the specular truncation rod, where the scattering vector \mathbf{Q} (difference between incident and diffracted X-rays) is normal to the graphite surface. These measurements probe the

topmost layers of the graphite crystal, irrespective of the positional order of these layers along the graphite surface.

A Kish graphite crystal (approximately 5mm in diameter and 0.2 mm thick) was used in these experiments. This was prepared by annealing at 1000 °C in flowing dry N₂ and was cleaved with Scotch tape just prior to the measurements.¹⁶ The X-ray diffraction measurements were conducted at beamline X20C at the National Synchrotron Light Source. An X-ray energy of 7.0 keV was used to limit penetration of the X-rays through the graphite. Approximately 30% of the intensity originated from the interface between the graphite on the sample holder. This is included in the analysis. Slits defined the incident beam size (0.09 x 1 mm²) and the diffracted beam resolution (0.12 degrees). Several variable parameters are used to modelling the data. These included an overall scale factor, the graphite surface roughness,¹⁵ adsorbed water coverage, and density of intercalated water/oxygen (between top and second carbon layer). The carbon-adsorbed water distance was fixed at 0.3 nm and the intercalated layer was assumed half-way between the graphite layers, since the fits were not very sensitive to these. Both the top and bottom surfaces were included in the modelling, but the bottom surface had an ideal termination.

Figure 2 shows the integrated diffracted intensity in high vacuum, laboratory air and water saturated air. As is apparent, the truncation rod profiles are all the same, to within experimental error. Thus, these data demonstrate that the near surface structure of the graphite is the same in high vacuum, laboratory air, and water saturated air. This *immediately* rules out any mechanism for low friction that involves an environmental

dependence of the basal-plane near surface structure and specifically shows the low friction does not result from shearing of weakened basal planes.

In order to determine near surface structure in the three environments, we have modelled the diffraction data shown in Fig. 2. Results from this analysis are shown in Fig. 3 for the laboratory air data. The solid line shows the best fit to the experimental data, and this fit adequately reproduces the data. In the model for this fit, there is a small expansion of the topmost graphite layer, roughness in the graphite surface, and a surface layer of physisorbed water (20 ± 10 % of a water monolayer); the best fit has no intercalation layer between the top and second graphite layers. Note that from our data we cannot determine the nature of the surface physisorbed layer; we have assumed that this is water, but it could equally well be an adsorbed hydrocarbon.

To assess the error bars, we have attempted to fit the data with the proposed low-friction models, specifically a near-surface intercalation layer and a surface chemisorbed layer. The dashed line in Fig. 3 shows the ‘fit’ with a 5% oxygen intercalation layer between the top and second layers, assuming a uniform expansion of the top-second graphite layer to accommodate the intercalation layer. This does not adequately fit the data, missing significantly near 2.3 \AA^{-1} . Since complete intercalation in graphite results in a large expansion of the graphite layer spacing (to 0.5-0.6 nm),¹⁷ it is possible that rather than a uniform expansion of the top layer spacing, a low density near surface intercalation layer would cause a large variation in the top-second layer graphite spacing (e.g, tent-poles). Incorporating this into the model fit only makes the ‘fit’ significantly worse (not shown for clarity). Thus, from this analysis, we conclude that the intercalation layer, if any, is $0 \pm 5\%$ of a graphite monolayer. Turning to the surface chemisorbed layer

model, the dot-dashed line shows the ‘fit’ with 10% chemisorbed oxygen (or water) layer and a consequent 0.025 nm expansion of the top-second graphite spacing. This completely fails to adequately describe the data; we conclude that there is no chemisorbed layer (<5% of a graphite monolayer) and no large (>0.01 nm) top-layer expansion. Note that the difference between a chemisorbed and physisorbed layer is the distance between the basal-plane and adsorbed layer. This is approximately 0.3 and 0.15 nm for chemisorption and physisorption, respectively.^{18,19} The analysis of the vacuum and water saturated air data are quite similar to analysis for the laboratory air data in Fig. 3, but are not shown here because of limited space. In all cases, we find a small expansion of the top graphite layer (from 0.335 nm in bulk graphite to 0.344 ± 0.005 nm).

Our diffraction results have demonstrated that, within the limits of experimental error, there is no change in the interlayer spacing of graphite basal planes near the surface as the outgassed graphite sample is exposed to ambient and humid air environments. This refutes the hypothesis that the low friction behavior of graphite in air is due to the weakening of binding force between basal planes near the surface by either intercalation⁴ or basal-plane chemisorption (π -bond etching),⁶ thereby facilitating the shear of the lattice. Hence, the original lattice-shear model¹ or its variants⁴ are not the prevalent mechanism in the context of friction. By refuting the lattice-shear model, our evidence lends strong support to the alternate explanation initially proposed by Deacon and Goodman:⁷ the graphite basal plane has intrinsically low surface energy,^{8,11} but vapor molecules are required to saturate dangling bonds at edge sites to maintain the low-friction behavior.⁹

This research was carried out in part at the National Synchrotron Light Source, Brookhaven National Laboratory, which is supported by the U.S. Department of Energy, Division of Materials Sciences and Division of Chemical Sciences, under Contract No. DE-AC02-98CH10886. Portions of this research were carried out at the Stanford Synchrotron Radiation Laboratory, a national user facility operated by Stanford University on behalf of the U.S. Department of Energy, Office of Basic Energy Sciences. We thank Ben Ocko for the use of his vacuum chamber and Mathew Mate for his critical comments and suggestions.

LIST OF REFERENCES

1. W. H. Bragg, in *An Introduction to Crystal Analysis* (G. Bell and Sons, London, 1928), p. 64.
2. D. Ramadanoff and S. W. Glass, *Trans. AIEE* **63**, 825 (1944).
3. R. H. Savage and D. L. Schaeffer, *J. Appl. Phys.* **27**, 136 (1956).
4. G. W. Rowe, *Wear* **3**, 274 (1960).
5. R. D. Arnell and D. G. Teer, *Nature* **218**, 1155 (1968).
6. P. J. Bryant, P. L. Gutshall, and L. H. Taylor, *Wear* **7**, 118 (1964).
7. R. F. Deacon and J. F. Goodman, *Proc. R. Soc. Lond. A* **243**, 464 (1958).
8. J. Skinner, N. Gane, and D. Tabor, *Nature* **232**, 195 (1971).
9. J. K. Lancaster and J. R. Pritchard, *J. Phys. D: Appl. Phys.* **14**, 747 (1981).
10. B. K. Yen and T. Ishihara, *Carbon* **34**, 489 (1996).
11. I. C. Roselman and D. Tabor, *J. Phys. D: Appl. Phys.* **9**, 2517 (1976).
12. J. W. Midgley and D. C. Teer, *Nature* **189**, 735 (1961).
13. B. Bhushan, in *Tribology and Mechanics of Magnetic Storage Devices* (Springer-Verlag, New York, 1990), p. 598.
14. K. M. Teo and K. Lafdi, *Tribol. Trans.* **44**, 664 (2001).
15. J. Als-Neilsen and D. McMorrow, in *Elements of Modern X-ray Physics*. (Wiley, New York, 2001), p. 135.
16. M. F. Toney, R. D. Diehl, and S. C. Fain, *Phys. Rev. B* **27**, 6413 (1983).
17. M. S. Dresselhaus and G. Dresselhaus, *Adv. Phys.* **51**, 1 (2002).

18. We have found no papers giving bond lengths for chemisorbed water or hydrocarbons on basal-plane graphite. Thus, we use a spacing of 0.15 nm, the approximate C-O bond length.

19. The position of the physisorbed water is estimated from measurements on similar sized atoms physisorbed on graphite (C. G. Shaw, S. C. Fain, M. D. Chinn, and M. F. Toney, *Surf. Sci.* **97**, 128 (1980)).

LIST OF FIGURES

Fig. 1. Schematic of graphite surface (perspective view from the side) showing ideal structure (a), physisorbed water layer on graphite (b), chemisorbed water layer on graphite (c), and intercalated layer (d). Cases (c) and (d) have a significant expansion in top layer distance. The orientation of the water is schematic only; we have no empirical evidence for its orientation.

Fig. 2. Integrated intensities as a function of scattering vector. The squares, circles, and diamonds are for lab air, 100% humid air, and high vacuum, respectively. The error bars are a result of a large diffuse background from the graphite crystal mount and roughness in the graphite surface.

Fig. 3. Integrated intensities as a function of scattering vector for lab air. The circles show the data and the solid line is the best fit. The dot-dashed line (which misses the data between about 2.0 and 2.5 \AA^{-1}) is for an intercalation layer of oxygen (or water) with a coverage of 5% of a graphite layer and a graphite top-layer spacing of 0.36 nm (compared to 0.335 nm in bulk). The dashed line (which misses the data near 2.5 \AA^{-1}) is for a top graphite layer spacing of 0.36 nm with a chemisorbed layer (coverage of 10% of a graphite layer at a height of 0.15 nm above the top basal plane). These fail to describe our data.

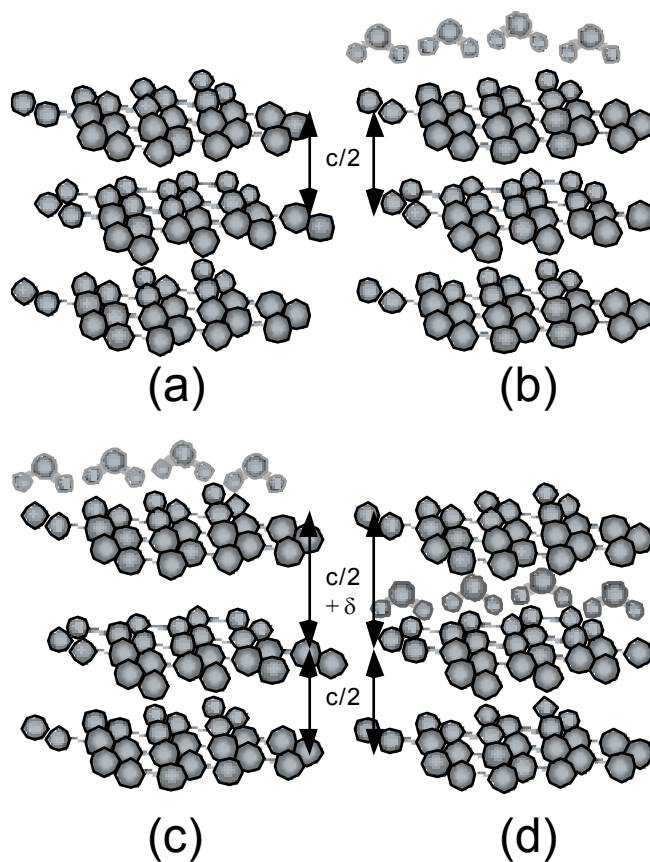


Fig. 1. Schematic of graphite surface (perspective view from the side) showing ideal structure (a), physisorbed water layer on graphite (b), chemisorbed water layer on graphite (c), and intercalated layer (d). Cases (c) and (d) have a significant expansion in top layer distance. The orientation of the water is schematic only; we have no empirical evidence for its orientation.

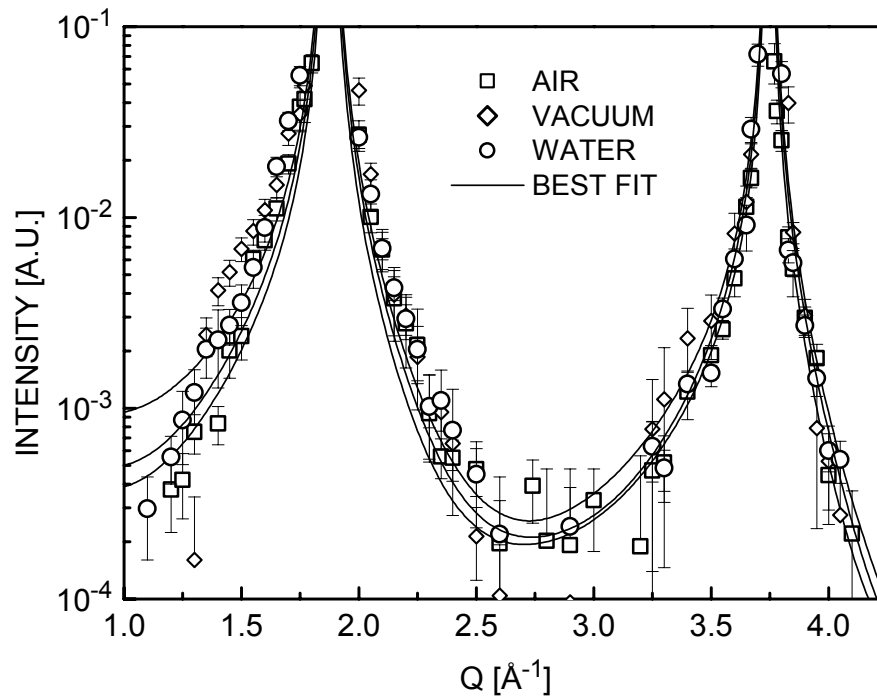


Fig. 2. Integrated intensities as a function of scattering vector. The squares, circles, and diamonds are for lab air, 100% humid air, and high vacuum, respectively. The error bars are a result of a large diffuse background from the graphite crystal mount and roughness in the graphite surface.

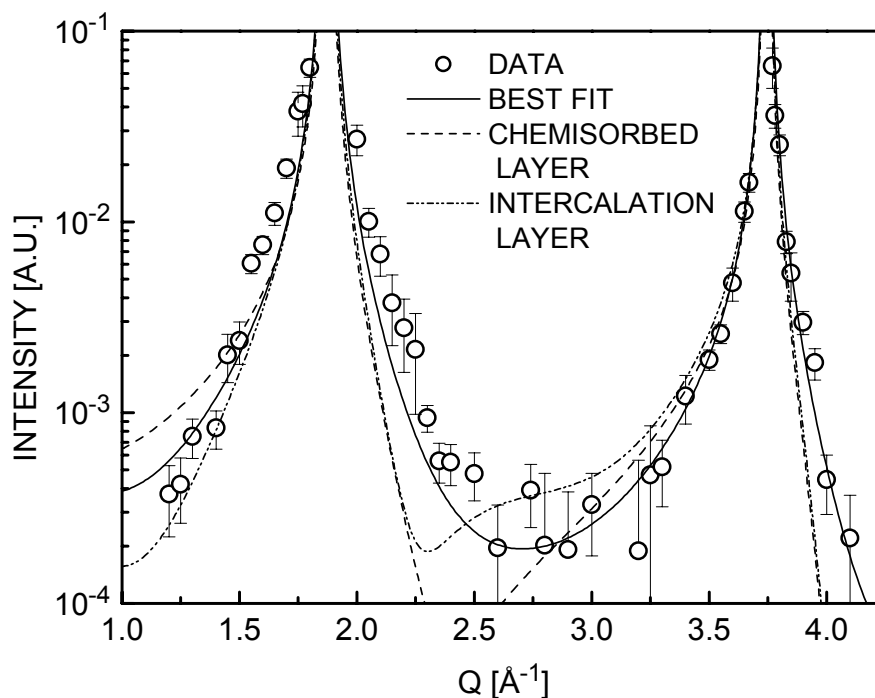


Fig. 3. Integrated intensities as a function of scattering vector for lab air. The circles show the data and the solid line is the best fit. The dot-dashed line (which misses the data between about 2.0 and 2.5 \AA^{-1}) is for an intercalation layer of oxygen (or water) with a coverage of 5% of a graphite layer and a graphite top-layer spacing of 0.36 nm (compared to 0.335 nm in bulk). The dashed line (which misses the data near 2.5 \AA^{-1}) is for a top graphite layer spacing of 0.36 nm with a chemisorbed layer (coverage of 10% of a graphite layer at a height of 0.15 nm above the top basal plane). These fail to describe our data.